Steady State Transpiration Cooling System in Ni-Cr Open-Cellular Porous Plate

P. Amatachaya, P. Khantikomol, R. Sangchot, and B. Krittacom

Abstract—The steady-state temperature for one-dimensional transpiration cooling system has been conducted experimentally and numerically to investigate the heat transfer characteristics of combined convection and radiation. The Nickel –Chrome (Ni-Cr) open-cellular porous material having porosity of 0.93 and pores per inch (PPI) of 21.5 was examined. The upper surface of porous plate was heated by the heat flux of incoming radiation varying from 7.7 - 16.6 kW/m^2 whereas air injection velocity fed into the lower surface was varied from 0.36 - 1.27 m/s, and was then rearranged as Reynolds number (Re). For the report of the results in the present study, two efficiencies including of temperature and conversion efficiency were presented. Temperature efficiency indicating how close the mean temperature of a porous heat plate to that of inlet air, and increased rapidly with the air injection velocity (Re). It was then saturated and had a constant value at Re higher than 10. The conversion efficiency, which was regarded as the ability of porous material in transferring energy by convection after absorbed from heat radiation, decreased with increasing of the heat flux and air injection velocity. In addition, it was then asymptotic to a constant value at the Re higher than 10. The numerical predictions also agreed with experimental data very well.

Keywords—Convection, Open-cellular, Radiation, Transpiration cooling, Reynolds number

I. Introduction

TRANSPIRATION cooling or effusion cooling [1] is the process of injecting a fluid (Air) into a porous material which can be served as a very efficient cooling method for protecting solid surfaces that are exposed to high-heat-flux, high-temperature from environments such as in hypersonic vehicle combustors, rocket nozzle, gas turbine blades, and the structure of re-entry aerospace vehicles [1]–[5].

P. Amatachaya is an assistant professor in the Department of Mechanical Engineering, Rajamangala University of Technology Isan, 744 Suranaria Rd., Muang Nakhonrajasima, 30000, THAILAND (corresponding author, tel: +66-44-233-073; fax: +66-44-233-074; e-mail: pipatana.am@ rmuti.ac.th).

P. Khantikomol is a member in the Research and Development of Renewable Energy Laboratory (RDREL), Mechanical Engineering Department, Rajamangala University of Technology Isan, 744 Suranaria Rd., Muang Nakhonrajasima, 30000, THAILAND (e-mail: preecha@ rmuti.ac.th).

R. Sangchot is a assistant researcher in the Development in Technology of Porous Materials Research Laboratory (DITTO-Lab), Mechanical Engineering Department, Rajamangala University of Technology Isan, 744 Suranaria Rd., Muang Nakhonrajasima, 30000, THAILAND.

B. Krittacom is a lecturer in the Development in Technology of Porous Materials Research Laboratory (DITTO-Lab), Mechanical Engineering Department, Rajamangala University of Technology Isan, 744 Suranaria Rd., Muang Nakhonrajasima, 30000, THAILAND (e-mail: bundit.kr@ rmuti.ac.th).

The performance of this cooling system is governed by several parameters such as radiative properties of porous media, the volumetric heat transfer coefficient between the solid phase and fluid, fluid velocity and irradiation. Thus, the knowledge of parameters for the design of transpiration-cooled devices is classified into two main groups including the phenomena of fluid flow and heat transfer process within the porous plate.

There are a number of experimental works [6] – [8] and numerical studies [9] – [12] have been conducted on transpiration cooling system. However, most of previous studies were mainly intended to determine the effects of convection mode. There were only a few studies have taken into account the radiative heat transfer in the transpiration cooling system. Recently, P.-X. Jiang et al. [13] and K. Kamiuto et al. [14] investigated experimentally and analytically to extend the validation of numerical model. P.-X. Jiang et al. [13] found that the numerical results corresponded well with the experimental data including the surface temperature and heat transfer coefficients. However, their work still focused on the effects of convective heat transfer. Radiation mode was concerned in the investigation of K. Kamiuto et al. [14]. They reported that the agreement between theoretical prediction and experimental results was acceptable. Although K. Kamiuto and co-worker considered the radiation mode in the transpiration cooling system, the result was more emphasized on theoretical basis and the difference between theory and experiment still existed.As a result, the present research aimed to further explore experimentally and analytically the heat transfer phenomena bycombinining convection and radiation in the transpiration cooling system using open-cellular porous materials. Theoretical Analysis

Figure 1 shows the present model of a transpiration cooling system . The assumptions of the numerical model are similar to those of K. Kamiuto et al. [14]. However, some modification was made to improve the accuracy of prediction. The following assumptions were introduced for this analysis: 1) an open-cellular porous plate of thickness x_0 is placed horizontally; 2) the front surface of porous plate is uniformly irradiated by blackbody radiation at an equivalent temperature T_R (K), while the back surface is subject to uniform blackbody radiation at an inlet air temperature; 3) a low-temperature air is injected through the back surface of porous plate and is assumed as a non-radiating body; 4) the porous medium is gray and is capable of emitting, absorbing and anisotropically scattering thermal radiation; 5) the porous medium is non-catalytic; 6) the physical properties depend on temperature which is different from the assumption used in [14]; 7) the heat transfer within the porous plate is in an one-dimensional steady-state; and 8) the behavior of air flow within a porous plate is under local and non-thermal equilibrium condition.
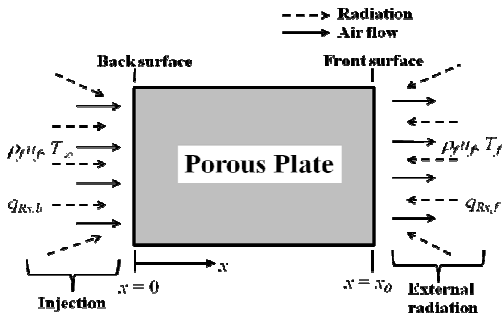
Fig. 1 The theoretical model and coordinate of a transpiration cooling system

Under these assumptions, the continuity equation is given by:

$$\frac{\partial (\rho_f u_f)}{\partial x} = 0 , \tag{1}$$

where ρ_f, u_f and x are density of a gas phase or cooled air (kg/m^3), air flow velocity (m/s) and coordinate in the flow direction (m) respectively.

The governing energy equations for the gas and the solid phases (porous plate) may be written as follows:

$$\rho_f u_f C_f \frac{\partial T_f}{\partial x} = \phi \frac{\partial}{\partial x}\left(k_f \frac{\partial T_f}{\partial x}\right) - h_v \left(T_f - T_s\right) , \tag{2}$$

$$\frac{1}{3}(1-\phi)\frac{\partial}{\partial x}\left(k_s \frac{\partial T_s}{\partial x}\right) + h_v \left(T_f - T_s\right) - \frac{\partial q_{Rx}}{\partial x} = 0 , \tag{3}$$

$$\frac{\partial q_{Rx}}{\partial x} = 4\beta(1-\omega)\left(\sigma T_s^4 - \frac{G}{4}\right). \tag{4}$$

Where C_f is the isobaric specific heat capacity (J/kg.$^{\circ}$C), σ is Stefan–Boltzmann constant (=5.67 × 10^{-8} W·m^{-2}·K^{-4}), G is incident radiation (W/m^2), ϕ is the porosity, h_v is the volumetric heat transfer coefficient between the gas and solid phases (W/m^3.$^{\circ}$C), β is the scaled extinction coefficient (m^{-1}), and ω is the scaled albedo. Modeling of last four physical properties was summarized in [15]. k_f and k_s are the thermal conductivity of a gas and solid phases, and T_f and $\underline{T_s}$ are temperature of gas and solid phases, respectively .

The G represents the incident radiation and q_{Rx} denotes as the net radiative heat flux in the flow direction. These quantities can be determined from the equation of transfer. Once the radiation field is specified, the quantities G and q_{Rx} can be readily evaluated. The radiative heat equation of the present research is solved by the P_1 approximation [16] and is written as:

$$\frac{dq_{Rx}}{dx} + (1-\omega)\beta(G - 4\sigma T_s^4) = 0 , \tag{5}$$

$$\frac{dG}{dx} + 3(1-\omega\tilde{g})\beta q_{Rx} = 0 , \tag{6}$$

where $\tilde{g}$ is asymmetric factor of scattering phase function.

The boundary conditions for (2), (3) and (4) are given as follows:

$$x = 0 : \quad T_f = T_\infty , \; \frac{\partial T_s}{\partial x} = 0, \; G - 2q_{Rx} = 4\sigma T_\infty^4 , \tag{7}$$

$$x = x_0 : \quad \frac{\partial T_f}{\partial x} = \frac{\partial T_s}{\partial x} = 0 , \; G + 2q_{Rx} = 4\sigma T_R^4 \tag{8}$$

Where T_∞ and T_R are the ambient temperature (K) and equivalent blackbody temperature of radiation source (K) respectively.

For convenience of calculations, the governing equations and associated boundary equations are transformed into dimensionless forms, and then the dimensionless equations are solved numerically using an implicit difference method. For solving the equation of transfer with the P_1 equations, and calculations of the T_f and T_s, the porous plate is divided into 200 equally spaced increments, whereas the optical thickness is divided into 400 equally spaced increments. To obtain the solutions of T_f and T_s, G or q_{Rx} are first determined based on an the assumption of temperature profile, and then the quantities of G and q_R are gained by solving equation of transfer or the P_1 equations at staggered lattice points [16]. Once G is obtained, the finite difference equations for T_f and T_s can be solved readily by Gaussian elimination. Thereafter, the derived solutions of T_f and T_s are substituted into the equation of transfer or the P_1 equations and the energy equations to get new solutions of these quantities; similar calculations are repeated until the following convergence criterion is satisfied: $\left|(Q^{(n)} - Q^{(n-1)})/Q^{(n)}\right| < 10^{-5}$.

Here, Q represents T_f, T_s, G or q_{Rx}, and n is time interval of calculation. After obtaining the T_f, T_s and G, two efficiencies, temperature efficiency (η_T) and conversion efficiency (η_C) are evaluated as follows:

$$\eta_T = \frac{\left[T_R - (T_{s,x=0} - T_{s,x=x_0})/2\right]}{T_R - T_\infty} . \tag{9}$$

$$\eta_C = \frac{\rho_f C_{Pf} u_f \left(T_{f,x=x_0} - T_{f,x=0}\right)}{q_{Rx,f}} . \tag{10}$$

II. EXPERIMENTAL APPARATUS AND PROCEDURE

A. Experimental Apparatus

Figure 2 shows a schematic diagram of the present experimental apparatus. The experimental set-up was constructed similar to that of Kamiuto et al. [14], but the double-tube heat exchanger was installed at the air inlet to keep air temperature at 25 – 30 $^{\circ}$C when it reached the back surface of the porous plate. Therefore, the present transpiration cooling system consisted of 4 sections including heat exchanger, inlet

air, porous medium, and radiation section. Air from a blower, that was used as the transpiration gas, was blown through the heat-exchanger and measured the flow rate using a rotermeter. The air was then flowed upward through a stainless pipe (0.01m inner diameter and 0.6m high) instead of acrylic pipe as in Kamiuto et al. [14]. A porous plate made of Ni-Cr (Ni/80 wt% and Cr/20 wt%) was placed on the top of the stainless pipe. The physical characteristics of the examined porous plate were summarized in table 1. Four 250-W infrared lamps were aligned above the porous plate to irradiate the heat into the upper surface of the plate. The amount of radiant energy was measured using heat flux sensor manufactured by Hukesflux Thermal Sensor, model HFP01-05. The intensity of the infrared lamps was regulated manually from 150 V to 250 V; thus the radiative heat flux was varied from 7.7 kW/m^2 to 16.6 kW/m^2.
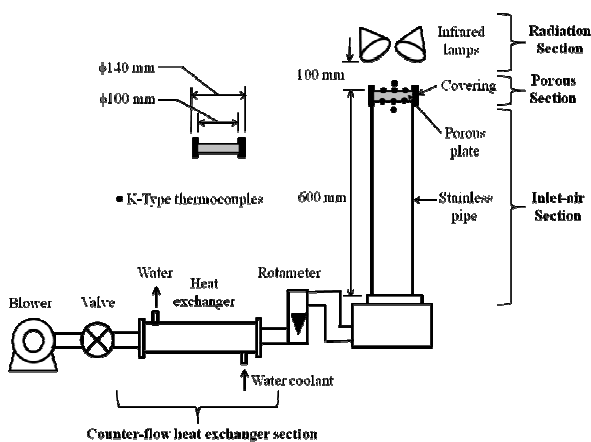

Fig. 2 Schematic diagram of the exponential apparatus

B. Experimental Procedure

The experimental procedures of the present cooling system was also similar to those of Kamiuto et al. [14]. After the infrared lamps were switched on, it took about 40 - 60 minutes for the porous plate to attain a steady-state of the temperatures. Six type-K thermocouple elements (0.0003m diameter) were adhered on the upper and lower surfaces of the porous plate. Inlet and outlet air temperature were measured using type-K sheathed thermocouples. The air flow rates were varied from 0.36 m/s to 1.27 m/s.

TABLE I
PHYSICAL CHARACTERISTICS OF A NICKEL-CHROME POROUS MATERIAL

Properties	Symbol	Quantity
porosity	ϕ	0.93
pore per inch	PPI	21
thickness	x_0	0.01 m
extinction coefficient	β	247.6 m^{-1}
optical thickness	τ	2.828

III. RESULTS AND DISCUSSION

A. Effects of Air Flow Velocity on Temperature Profiles

Figure 3 illustrated the theoretical results of the temperature profiles of the gas and the solid phases inside the Ni-Cr porous plate, under the condition of irradiated heat flux $q_{Rx,f}$ = 12.5 kW/m^2. The measured mean surface temperatures of the porous plate is indicated by black symbols, while the calculated results for gas (T_f) and solid phase (T_s) are presented using the solid and dot lines respectively. The temperature of both phases increase along the porous lengthbecause the incident radiation from the infrared lamps was emitted down to the front surface. For a fixed position of the thickness x, the temperature profiles of T_f and T_s deceased as the air velocity (u_f) increased owing to the effects of a higher convective heat transfer [11]. Agreement between the predicted and the experimental results at the exit region (x = 10 mm) or front surface was satisfactory.
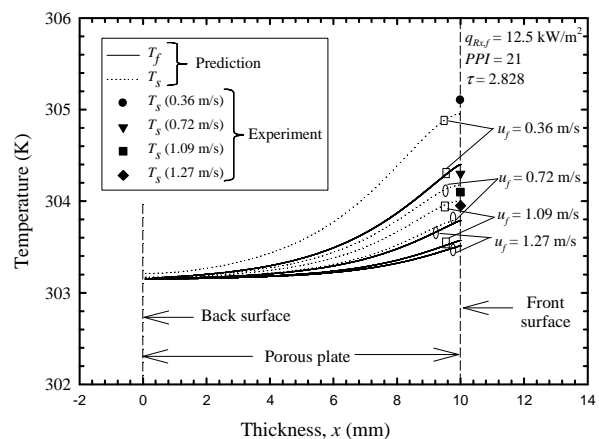

Fig. 3 Profiles of the gas and solid phase temperatures within the Ni-Cr open-cellular plate for the effect of air flow velocity (The symbols indicate the present experimental data)

B. Effects of Heat Flux on Temperature Profiles

Figure 4 illustrates the theoretical results of the temperature profiles of the gas and solid phases inside the Ni-Cr porous plate under the condition of air flow velocity (u_f) of 0.72 m/s. The temperatures of both phases (T_f and T_s) gradually increased along the porous length due to incident radiation from the infrared lamps. For a fixed position of thickness x, the temperature profiles of T_f and T_s increased with radiative heat flux ($q_{Rx,f}$) because porous medium absorbed a higher radiant energy from the infrared lamps. Agreement between the predicted results and the experimental data at the exit region ($x \approx$ 10 mm) was satisfactory.
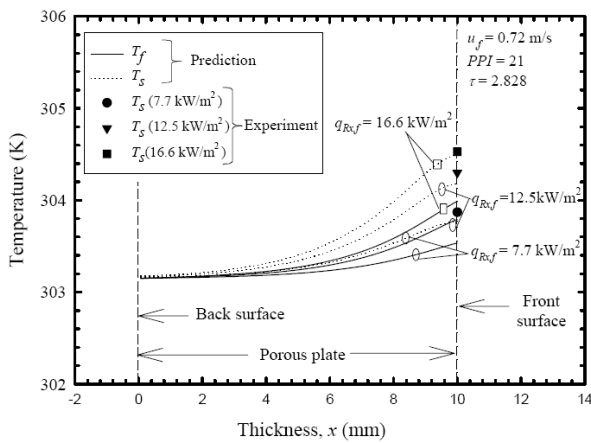
Fig. 4   Profiles of the gas and solid phase temperatures within the Ni-Cr open-cellular plate for the effect of heat flux (The symbols indicate the present experimental data)

C. The Temperature Efficiency

Figure 5 shows variations in the temperature efficiency η_T against Reynols number (Re). In this study, Re represents the air flow velocity which is defined by using $\rho_f u_f D_s/\mu_f$, where μ_f is viscosity of a gas phase (Pa·s), and D_s is the equivalent strut diameter (m) as described in Krittacom [15]. The experimental results are shown using symbols, while the numerical results are indicated by using the lines. The figure illustrated that the η_T increased rapidly with Re and then asymptotic to a constant value for the Re higher than 10. However, at a fixed Re, the η_T decreased with the increase of the incident radiation. For the Re higher than 10, the values of η_T were greater than 0.9. This indicated that the average temperature of the porous plate was very close to the average heat shield temperature and inlet air temperature. Agreement between theory and experiment was acceptable which indicated the validity of the present numerical model.

D. The Conversion Efficiency

Figure 6 shows variations in the conversion efficiency η_C against Re. The results demonstrated that the η_C increased slightly with Re and was asymptotic to a constant value for the Re higher than 10 in which the η_C values were varied in the range of 75% to 80%. For a fixed value of Re, η_C increased with incident radiation ($q_{Rx,f}$) because the porous media absorbed energy from a higher heat flux and then transferred via convection through the cooled-air flow. Thus, the ability of transferring energy of Ni-Cr open-cellular porous plate by convection after absorbing heat radiation decreased with the increasing of heat flux. Agreement between theory and experiment was acceptable.
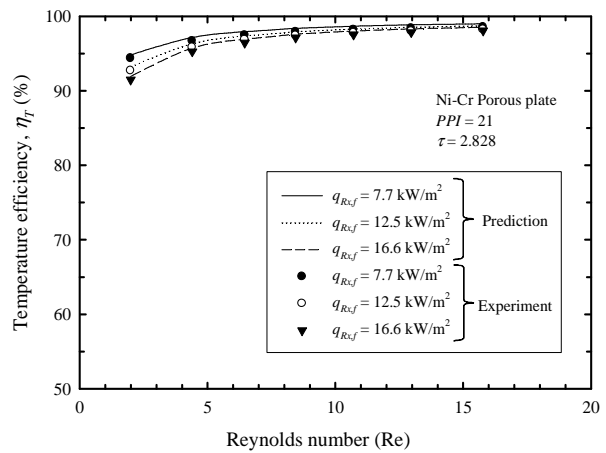

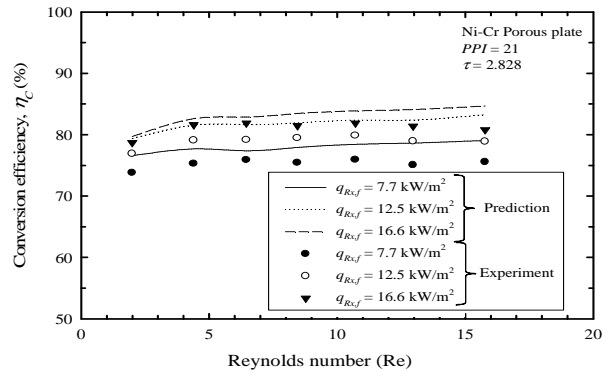Fig. 5   Comparison of predicted and measured temperature efficiency of the Ni-Cr open-cellular porous plate

Fig. 6   Comparison of predicted and measured conversion efficiency of the Ni-Cr open-cellular porous plate

IV.   CONCLUSION

The major conclusions that can be drawn from the present study are summarized as follows:

1) The temperature profiles of gas (T_f) and solid (T_s) phase deceased as air injection velocity (u_f) increased because of the effects of a higher convective heat transfer, whereas the profiles of both temperature increased with incident radiation ($q_{Rx,f}$) owing to the effects of higher radiant energy.

2) The temperature efficiency (η_T) rapidly increased with air injection velocity but was saturated at a constant value for Re greater than 10.

3) The conversion efficiency (η_C) of a Ni-Cr porous plate increased slightly with Re and was asymptotic to a constant value at $Re = 10$.

4) Agreement between the predicted results based on P_1 equations and experimental data was acceptable, thereby the validity of theoretical model was confirmed.

5) Incoming radiation from a radiative environment can be almost completely protected as long as the Re of the

open-cellular plate was about ten or higher. As a result, the transpiration cooling system as used in the present open-cellular porous plate should be designed for the Re = 10.

REFERENCES

[1] Grootenhuis, P., "The mechanism and application of effusion cooling", *Journal of the Royal Aeronautic Society*, vol. 63, pp. 73 – 89, Feb. 1959.

[2] Choi, S.H., Scotti, S.J., Song, K.D. and Ries, H., "Transpiring cooling of a scram-jet engine combustion chamber", *NASA AIAAA-97-2576*, 1997.

[3] Glass, D.E., Dilley A.D. and Kelly, H.N., "Numerical analysis of convection/transpiration cooling", *AIAA J Spacecraft Rockets*, vol. 38 no.1, pp. 15–20, 2001.

[4] Bayley, F.J. and Turner, A.B., "The heat transfer performance of porous gas turbine blades", *Aeronautical J*, vol. 72 (696), pp. 1087–1094, 1968.

[5] Bayley, F.J., "Transpiration cooled turbines", *Proc. Instn. Mech. Engineering*, vol. 185, no. 69/71, pp. 943-956, 1970.

[6] Duwez, P. and Wheeler, H.L., "Experimental study of cooling by injection of a fluid through a porous material", *Journal of Aeronautical Sciences*, vol. 15, pp. 509 – 521, Sep. 1948.

[7] Andrews, G.E. and Asere, A., "Transpiration cooling of gas turbine combustion chamber walls", *Institute of Chemical Engineering Symposium Series*, vol. 86, pp.1047-1056, 1984.

[8] Fu, X., Viskanta, R. and Gore, J.P. "Measurement and correlation of volumetric heat transfer coefficients", *Experimental and Thermal and Fluid Science*, vol. 17, no.4, pp.285-293, Aug. 1998.

[9] Kubota, H., "Thermal response of a transpiration-cooled system in a radiative and convective Environment", *Transaction of the ASME: Journal of Heat Transfer*, vol. 99, pp. 628 – 633, Nov. 1977.

[10] Eckert, E.R.G. and Cho, H.H., "Transition from transpiration to film cooling", *Int J Heat Mass Transfer*, vol. 37 (supplement 1), pp.3–8, Mar. 1994.

[11] Wolfersdorf, J.V., "Effect of coolant side heat transfer on transpiration", *Heat Mass Transfer*, vol. 41, pp.327-337, 2005.

[12] Andoh, Y.H., and Lips, B. "Prediction of porous walls thermal protection by effusion or transpiration cooling. An analytical approach", *Applied Thermal Energy*, vol. 23, no. 15, pp.1947-1958, Oct. 2003.

[13] Jiang, P.-X., Yu, L., Sun, J.-G., and Wang, J., "Experimental and numerical investigation of convection heat transfer in transpiration cooling", *Applied Thermal Engineering*, vol. 24, no. 8-9, pp.1271-1289, Jun. 2004.

[14] Kamiuto, K. "Thermal characteristics of transpiration cooling system using open-cellular porous materials in a radiative environment", *Int. J. Trans. Phenomena*, vol. 7, pp. 58-96, 2005, pp.62-68.

[15] Krittacom, B., *Studies on Thermal Characteristics of Open-Cellular Porous Burners*, Ph.D. Dissertation, Oita University, Japan, 2009.

[16] Kamiuto, K., Saito, S. and Ito, K., "Numerical model for combined conductive and radiative heat transfer in annular packed beds, *Numerical Heat Transfer*, Part A, vol. 23, pp.433-443, 1993.